*Anti-Infective Agents*, 2019, *17*, 50-65

RESEARCH ARTICLE

# Design, Synthesis and Biological Profiling of Novel Phenothiazine Derivatives as Potent Antitubercular Agents

Satheeshkumar Sellamuthu[1], Ashok Kumar[1], Gopal Nath[2] and Sushil Kumar Singh[1,*]

[1]*Pharmaceutical Chemistry Research Laboratory, Department of Pharmaceutical Engineering & Technology, Indian Institute of Technology (Banaras Hindu University), Varanasi-221005, India;* [2]*Department of Microbiology, Institute of Medical Sciences, Banaras Hindu University, Varanasi-221005, India*

ARTICLE HISTORY

Received: May 18, 2018
Revised: June 06, 2018
Accepted: July 11, 2018

*DOI:*
*10.2174/2211352516666180730121013*

**Abstract:** ***Background*:** Neuroleptic phenothiazines have been reported for antitubercular activity, but the unwanted side effect (antipsychotic activity) restricted their use as antitubercular drugs.

***Objective*:** The study aimed to carry out development of phenothiazine based antitubercular agents by modifying/removing the chemical group(s)/ linker(s) of chlorpromazine essential for exerting an antipsychotic effect.

***Methods*:** The designed molecules were filtered with a cut-off of docking score < 2.0 Kcal/mol against dopamine receptors, so that their binding with the receptor would be reduced to produce no/ less antipsychotic effect. The molecules were then synthesized and screened against *M. tuberculosis* H37Rv. They were further screened against a *gram*-positive (*S. aureus*) and a *gram*-negative (*E. coli*) bacterial strains to evaluate the spectrum of activity. The ability of the compounds to cross the blood-brain barrier (BBB) was also analyzed. The compounds were further examined for cytotoxicity ($CC_{50}$) against mammalian VERO cells.

***Results*:** Compounds **14p**, **15p** and **16p** were found to be the most effective against all the strains *viz. M. tuberculosis* H37Rv, *S. aureus* and *E. coli* with MIC of 1.56µg/ml, 0.98µg/ml and 3.91µg/ml, respectively. Further, BBB permeability was found to be diminished in comparison to chlorpromazine, which would ultimately reduce the unwanted antipsychotic activity. They were also found to be free from toxicity against VERO cells.

***Conclusion*:** The designed strategy, to enhance the antitubercular activity with concomitant reduction of dopamine receptor binding and BBB permeability was proved to be fruitful.

**Keywords:** Antibacterial, antitubercular, BBB permeability, cytotoxicity, molecular property, OSIRIS DataWarrior, phenothiazine

## 1. INTRODUCTION

Tuberculosis (TB) is a deadly infectious disease caused by the bacillus *Mycobacterium tuberculosis* (Mtb). It is the leading cause of mortality along with HIV worldwide [1]. The bacillus naturally affects the lungs to produce pulmonary TB, but can also affect other parts as well to cause extrapulmonary TB [2]. Out of 10.4 million new TB cases estimated in 2015, 60% of them were from six countries *i.e.* India, Indonesia, China, Nigeria, Pakistan and South Africa. In another estimate, 1.8 million people (1.4 million HIV-negative and 0.4 million HIV-positive) had died of the disease in 2015 [3]. In nutrient deprived and anaerobic conditions, Mtb develops a latent infection that in turn may transform into an active disease at any moment in lifetime. [4]. Hence, dormant/latent TB needs to be treated before its conversion into an active disease [5]. A large number of TB patients were accounted for drug resistance and 480 000 new cases of Multi-Drug Resistant Tuberculosis (MDR-TB) were reported in 2015 [3]. The treatment of MDR-TB lasts for 20 months, yet the success rate is not satisfactory [6]. The TB epidemic is further fuelled with the emergence of extensively drug-resistant TB (XDR-TB). The decade-old treatment regimen and poor efficacy of current TB drugs pose a grave threat to humanity. The infections caused by *E. coli* and *S. aureus* are also a matter of serious concern. Over 85% of urinary tract infections were caused by uropathogenic *E. coli* [7] and many life-threatening infections *viz*. pneumonia, bloodstream infections and surgical-site infections were caused by methicillin-resistant *S. aureus* (MRSA) [8]. Due to the failure of existing drugs to produce rapid cure of TB, re-engineering/repositioning of old families of drugs may be

*Address correspondence to this author at the Pharmaceutical Chemistry Research Laboratory, Department of Pharmaceutical Engineering & Technology, Indian Institute of Technology (Banaras Hindu University), Varanasi-221005, India; Tel: 0542-6702736/4; E-mail: sksingh.phe@iitbhu.ac.in

2211-3533/19 $58.00+.00 

rewarding. Phenothiazine class of drugs *viz*. chlorpromazine, trifluoperazine and thioridazine were reported for potent antitubercular activity but cognitive side effects limited their use in the treatment of TB [9-11]. Chlorpromazine and thioridazine were reported for their appreciable levels of antimicrobial activity, regardless of their antibiotic susceptibility. Thioridazine (TDZ), used safely over four decades for the treatment of psychosis, was also used to treat XDR-TB patients on a compassionate basis, in cases where other antibiotic therapies did not respond [12]. According to a report, 10 of 12 XDR-TB patients were cured with thioridazine treatment and the remaining 2 also responded favorably but were dropped out of the program [11]. When chlorpromazine was used as an adjuvant at a concentration that was least effective against MDR-TB, the activity of rifampicin and streptomycin steeply increased [13]. Therefore, there is potential to develop phenothiazine class of compounds as antitubercular agents.

The structure-activity (anti-psychotic) relationship of Chlorpromazine (CPZ) revealed that the dimethylamino (tailing) group linked through an alkyl connector at the tenth position and a halogen atom at the second position were necessary for antipsychotic activity [14, 15]. In the present study, we aimed to introduce definite modifications in chlorpromazine to increase the antitubercular activity with a concurrent reduction in unwanted effect. The approach is to remove/modify the pharmacophore/linker/tailing-group(s) of chlorpromazine, essential for antipsychotic activity. The molecules were designed by altering the pharmacophore, connector, as well as the tailing group of chlorpromazine to increase antitubercular activity with a concomitant reduction in unwanted binding to dopamine receptors. Phenothiazine pharmacophore was retained due to reported antitubercular efficacy [16]. The alkyl connector was modified to an acyl connector. The tailing group was also modified with different substituted phenylamines/ phenylpiperazines (Fig. **1**). Since the molecules were designed by altering chlorpromazine nucleus, they may also produce antipsychotic effect. Therefore, we virtually screened the designed molecules against the possible off-targets *viz.* dopamine D2 (PDB: 6CM4) and D3 (PDB: 3PBL) receptors through high-throughput virtual screening to avoid unwanted antipsychotic effect.

## 2. MATERIALS AND METHODS

### 2.1. Off-target Virtual Screening and Filtering of Designed Molecules

The designed molecules were screened against dopamine D2 (PDB: 6CM4) and D3 (PDB: 3PBL) receptors using Maestro 10.5.014 application (Schrödinger, LLC, USA, 2016-1). The whole process involved protein preparation, ligand preparation, receptor grid generation and finally ligand docking. The process of protein preparation and energy minimization of 6CM4 and 3PBL was performed using protein preparation wizard of Maestro. The active site amino acid residues were selected and receptor grid was generated encompassing these residues, using the grid generation module of Maestro. Ligands were then subjected to ligand preparation using the ligand preparation wizard in Maestro. During this, ionization and tautomeric states of ligands were generated using the Epic module. The prepared ligands were then screened against the energy minimized protein through high-throughput virtual screening in Schrodinger suite [17]. Docking score of ≤ 2.0 Kcal/mol was fixed as the cut-off, to filter the molecules having least interaction with dopamine receptors (D2 & D3).

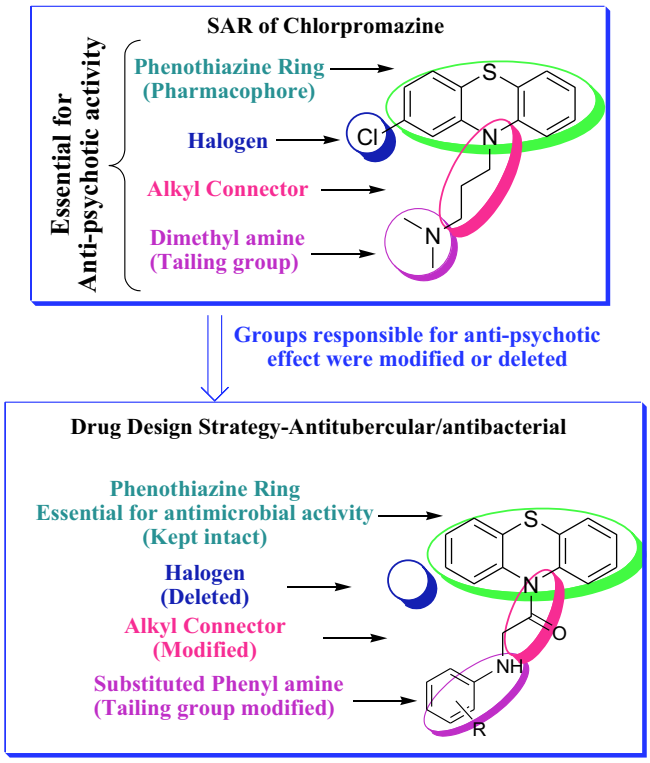


**Fig. (1).** Design strategy for phenothiazine based antitubercular and antibacterial agents.

### 2.2. Synthesis of 10H-phenothiazine (b)

Diphenylamine **(a)** (10g, 59.09mmol), elementary sulfur (3.78g, 118.18mmol), and iodine (0.74g, 5.90 mmol) were taken in RB flask with 1-2-dichlorobenzene as the solvent and heated at 180°C for 2 hours. The evolved hydrogen sulphide was trapped in an aqueous solution of NaOH. The solvent was removed under vacuum. The crude material was subjected to flash column chromatography ($SiO_2$, EtOAc:hexanes at 1:9), which afforded pure phenothiazine. It was recrystallized twice with aqueous ethanol to get light yellow crystals [18] (Scheme **1**).

Yield: 90%; MP: 181-183ºC; $^1$H-NMR (500 MHz, $CDCl_3$) δ (ppm): 7.533, 7.517 (d, J = 8 Hz, 2H, C1, C8-phenothiazine), 7.412-7.395 (dd, J = 8.5, 1.1 Hz, 2H, C4, C5-phenothiazine), 7.310-7.295 (td, J = 7.5, 1.1 Hz, 2H, C2, C7-phenothiazine), 7.224-7.195 (td, J = 7.5, 1.1 Hz, 2H, C3, C6-phenothiazine); $^{13}$C-NMR (125 MHz, $CDCl_3$) δ (ppm): 138.051, 133.405, 128.350, 127.619, 127.526, 126.738 (aromatic carbons); MS (ESI) m/z: 200.7 (M+1, 100%). Anal. Calcd for $C_{12}H_9NS$: C, 72.33; H, 4.55; N, 7.03; Found: C, 72.54; H, 4.57; N, 7.08 %.

### 2.3. Synthesis of 2-chloro-1-(10H-phenothiazin-10-yl) ethan-1-one (1p)

10H-phenothiazine **(b)** (10.0 g, 59.09 mmol) was taken in chloroform ($CHCl_3$) (150 mL) and cooled down to 0°C; fol-

lowing this, chloroacetyl chloride (6.0 mL, 75.2 mmol) was added dropwise and the reaction mixture was stirred for 12 hours at 37°C. It was then allowed to cool to room temperature and concentrated under reduced pressure to obtain a crude product. Water (100 mL) was added to it and extracted with dichloromethane (DCM) (2 × 100 mL). The organic layer was dried over anhydrous $Na_2SO_4$ and the solvent was evaporated to get pale white product [18] (Scheme **1**).

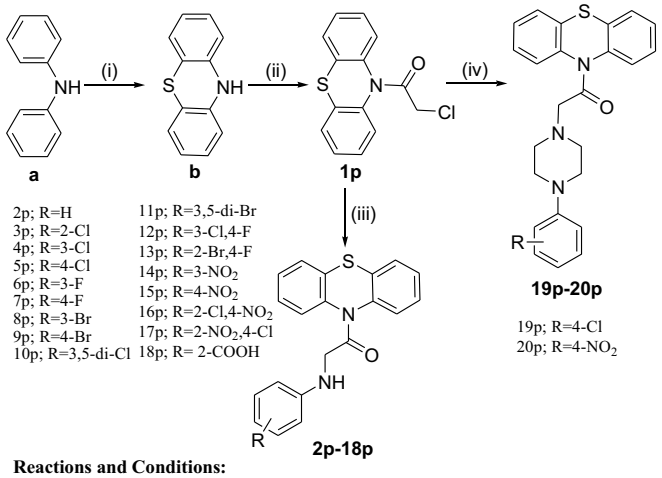


**Reactions and Conditions:**
(i) elementary sulphur, iodine, 1,2-dichlorobenzene, 180°C, 2h.
(ii) $CHCl_3$, cool 0°C, add chloro acetyl chloride, stirring 37°C, 10h.
(iii) corresponding phenylamine, $K_2CO_3$, THF, 67°C, reflux, 9-12h.
(iv) corresponding phenyl piperazine, $K_2CO_3$, PI, THF, 7-9h.

**Scheme 1.** Synthesis of phenothiazine derivatives.

Yield: 95%; MP: 111-113°C; $^1$H-NMR (500 MHz, $CDCl_3$) δ (ppm): 7.524, 7.508 (d, J = 8 Hz, 2H, C1, C8-phenothiazine), 7.403-7.386 (dd, J = 7.5, 1.1 Hz, 2H, C4, C5-phenothiazine), 7.301-7.286 (td, J = 7.5, 1.1 Hz, 2H, C2, C7-phenothiazine), 7.215-7.186 (td, J = 7.5, 1.1 Hz, 2H, C3, C6-phenothiazine), 4.111 (s, 2H, Methylene-$CH_2$); $^{13}$C NMR (125 MHz, $CDCl_3$) δ (ppm): 165.717 (C=O), 138.111, 133.817, 128.353, 127.626, 127.529, 126.743 (aromatic carbons), 41.994 (methylene carbon); MS (ESI) m/z: 277.5 (m+2, 25%), 276. 5 (m+1, 75%). Anal. Calcd for $C_{14}H_{10}ClNOS$: C, 60.98; H, 3.66; N, 5.08; Found: C, 61.24; H, 3.69; N, 5.03%.

### 2.4. Synthesis of Phenothiazine Derivatives (2p-20p)

2-Chloro-1-phenothiazine-10-yl-ethanone **(1p)** (0.2g, 0.73 mmol), potassium carbonate ($K_2CO_3$) (0.2 mg, 1.45 mmol), potassium iodide (KI) (0.06 mg, 0.365 mmol) and corresponding phenyl amines/ phenyl piperazines (1.09 mmol) were taken in 10 mL tetrahydrofuran (THF) and refluxed at 67°C for 7-12 hours. The crude material was subjected to flash column chromatography (SiO2, EtOAc:hexane at 1:9 to 4:6 ratios) to obtain different phenothiazine derivatives (Scheme **1**).

### 2.5. 1-(10H-phenothiazin-10-yl)-2-(phenylamino)ethan-1-one (2p)

Yield: 78%; MP: 145-147°C; $^1$H-NMR (500 MHz, $CDCl_3$) δ (ppm); 7.612, 7.596 (d, J=7.5 Hz, 2H, C1, C8-phenothiazine), 7.548, 7.533 (d, J=7.5 Hz, 2H, C4, C5-phenothiazine), 7. 483-7.425 (td, J=14, 7.5 Hz, 2H, C2, C7-phenothiazine), 7.381-7.325 (td, J=14, 7.5 Hz, 2H, C3, C6-phenothiazine), 7.105-7.089 (t, J=8 Hz, 2H, C3, C5-phenyl), 6.818-6.802 (t, J=8 Hz, 2H, C2, C6-phenyl), 6.634-6.618 (t, J=8 Hz, 1H, C4-phenyl), 3.966 (s, 2H, methylene-$CH_2$), 3.497 (s, 1H, NH); $^{13}$C-NMR (125 MHz, $CDCl_3$) δ: 167.328 (C=O), 145.043, 139.997, 134.651, 130.825, 128.174, 127.079, 126.653, 123.138, 120.367, 115.552 (Aromatic carbons), 55.672 (methylene carbon); MS (ESI) *m/z*: 333.2 (M+1, 42.1%); Anal. Calcd for $C_{20}H_{16}N_2OS$: C, 72.26; H, 4.85; N, 8.43; Found: C, 72.41; H, 4.87; N, 8.47 %.

### 2.6. 2-((2-chlorophenyl)amino)-1-(10H-phenothiazin-10-yl)ethan-1-one (3p)

Yield: 75%; MP: 154-156ºC; $^1$H-NMR (500 MHz, $CDCl_3$) δ; 7.574, 7.558 (d, J=8 Hz, 2H, C1, C8-phenothiazine), 7.442-7.427 (d, J=7.5 Hz, 2H, C4, C5-phenothiazine), 7.340-7.307 (td, J=7.5, 1.5 Hz, 2H, C2, C7-phenothiazine), 7.253-7.220 (m, 3H, C3, C6-phenothiazine, C3-phenyl), 7.153-7.127 (t, J=6.5 Hz, 1H, C4-phenyl), 6.718, 6.701 (d, J=8.5 Hz, 1H, C6-phenyl, 6.653-6.627 (t, J=6.5 Hz, 1H, C5-phenyl), 4. 175 (s, 2H, methylene-$CH_2$) 3.864 (s, 1H, NH); $^{13}$C-NMR (125 MHz, $CDCl_3$) δ: 168.005 (C=O), 145.971, 140.135, 134.883, 131.099, 130.455, 128.238, 127.654, 126.342, 123.214, 121.535, 119.958, 114.822 (Aromatic carbons), 53.526 (methylene carbon); MS (ESI) *m/z*: 368.5 (M+2, 25%), 367.6 (M+1, 74%); Anal. Calcd for $C_{20}H_{15}ClN_2OS$: C, 65.48; H, 4.12; N, 7.64; Found: C, 65.61; H, 4.13; N, 7.67 %.

### 2.7. 2-((3-chlorophenyl)amino)-1-(10H-phenothiazin-10-yl)ethan-1-one (4p)

Yield: 82%; MP: 155-156ºC; $^1$H-NMR (500 MHz, $CDCl_3$) δ; 7.577, 7.561 (d, J=8 Hz, 2H, C1, C8-phenothiazine), 7.452-7.433 (dd, J=9.5, 1.5 Hz, 2H, C4, C5-phenothiazine), 7.348-7.314 (td, J=7.5, 1.5 Hz, 2H, C2, C7-phenothiazine), 7.261-7.230 (td, J=6, 1.5 Hz, 2H, C3, C6-phenothiazine), 7.014-6.986, (t, J=7 Hz, 1H, C5-phenyl), 6.718, 6.702 (d, J=8 Hz, 1H, C4-phenyl), 6.652 (s, 1H, C2-phenyl), 6.411, 6.395 (d, J= 8 Hz, 1H, C6-phenyl), 4.177 (s, 2H, Methylene $CH_2$), 3.928 (s, 1H, NH); $^{13}$C-NMR (125 MHz, $CDCl_3$) δ: 168.011 (C=O), 147.975, 140.141, 134.891, 135.455, 130.457, 128.246, 127.066, 126.336, 123.212, 119.995, 115.902, 112.549 (Aromatic carbons), 53.526 (methylene carbon); MS (ESI) *m/z*: 368.5 (M+2, 25%), 367.4 (M+1, 75%); Anal. Calcd for $C_{20}H_{15}ClN_2OS$: C, 65.48; H, 4.12; N, 7.64; Found: C, 65.57; H, 4.11; N, 7.68%.

### 2.8. 2-((4-chlorophenyl)amino)-1-(10H-phenothiazin-10-yl)ethan-1-one (5p)

Yield: 79%; MP: 155-157ºC; $^1$H-NMR (500 MHz, $CDCl_3$) δ; 7.645, 7.629 (d, J=8 Hz, 2H, C1, C8-phenothiazine), 7.521, 7.506 (d, J=7.5 Hz, 2H, C4, C5-phenothiazine), 7.448-7.415 (td, J=15, 1.5 Hz, 2H, C2, C7-phenothiazine), 7.550-7.517 (td, J=15, 1.5 Hz, 2H, C3, C6-phenothiazine), 7.112, 7.098 (d, J=6.5 Hz, 2H, C3, C5-phenyl), 6.622, 6.604 (d, J=8.5 Hz, 2H, C2, C6-phenyl), 4. 013 (s, 2H, methylene-$CH_2$) 3.582 (1H, NH); $^{13}$C-NMR (125 MHz, $CDCl_3$) δ: 166.972 (C=O), 144.783, 139.251, 133.918, 130.582, 128.733, 127.915, 126.626, 125.125, 122.288, 115.161 (Aromatic carbons), 52.651 (methylene carbon); MS (ESI) *m/z*: 368.5 (M+2, 24%), 367.6 (M+1, 75%); Anal.

Calcd for $C_{20}H_{15}ClN_2OS$: C, 65.48; H, 4.12; N, 7.64; Found: C, 65.65; H, 4.13; N, 7.65%.

### 2.9. 2-((3-fluorophenyl)amino)-1-(10H-phenothiazin-10-yl)ethan-1-one (6p)

Yield: 67%; MP: 151-153ºC, $^1$H-NMR (500 MHz, $CDCl_3$) δ; 7.575, 7.559 (d, J=8 Hz, 2H, C1, C8-phenothiazine), 7.451-7.432 (dd, J=9.5, 1.5 Hz, 2H, C4, C5-phenothiazine), 7.351-7.317 (td, J=7.5, 1.5 Hz, 2H, C2, C7-phenothiazine), 7.258-7.227 (td, J=6, 1.5 Hz, 2H, C3,C6-phenothiazine), 7.009-6.981, (t, J=7 Hz, 1H, C5-phenyl), 6.720,6.704 (d, J=8 Hz, 1H, C4-phenyl), 6.659 (s, 1H, C2-phenyl), 6.408, 6.392 (d, J= 8 Hz, 1H, C6-phenyl), 4.198 (s, 2H, Methylene $CH_2$), 3.935 (s, 1H, NH); $^{13}$C-NMR (125 MHz, $CDCl_3$) δ: 168.023 (C=O), 147.805, 141.041, 135.991, 134.432, 130.762, 128.421, 126.973, 126.181, 124.002, 120.086, 116.109, 112.330 (Aromatic carbons), 53.842 (methylene carbon); MS (ESI) *m/z*: 351.3 (M+1, 78%); Anal. Calcd for $C_{20}H_{15}FN_2OS$: C, 68.55; H, 4.31; N, 7.99; Found: C, 68.62; H, 4.33; N, 8.03%.

### 2.10. 2-((4-fluorophenyl)amino)-1-(10H-phenothiazin-10-yl)ethan-1-one (7p)

Yield: 62%; MP: 152-154ºC; $^1$H-NMR (500 MHz, $CDCl_3$) δ; 7.634, 7.618 (d, J=8 Hz, 2H, C1, C8-phenothiazine), 7.525, 7.510 (d, J=7.5 Hz, 2H, C4, C5-phenothiazine), 7.452-7.417 (td, J=15, 1.5 Hz, 2H, C2, C7-phenothiazine), 7.547-7.514 (td, J=15, 1.5 Hz, 2H, C3, C6-phenothiazine), 7.152, 7.138 (d, J=7 Hz, 2H, C3, C5-phenyl), 6.628, 6.610 (d, J=8.5 Hz, 2H, C2, C6-phenyl), 4.102 (s, 2H, methylene-$CH_2$) 3.529 (s, 1H, NH); $^{13}$C-NMR (125 MHz, $CDCl_3$) δ: 167.041 (C=O), 144.808, 139.346, 133.537, 130.591, 128.905, 127.611, 126.584, 125.222, 122.169, 115.184 (Aromatic carbons), 53.563 (methylene carbon); MS (ESI) *m/z*: 351.3 (M+1, 78%); Anal. Calcd for $C_{20}H_{15}FN_2OS$: C, 68.55; H, 4.31; N, 7.99; Found: C, 68.68; H, 4.25; N, 8.02%.

### 2.11. 2-((3-bromophenyl)amino)-1-(10H-phenothiazin-10-yl)ethan-1-one (8p)

Yield: 58%; MP: 176-179ºC, $^1$H-NMR (500 MHz, $CDCl_3$) δ: 7.581, 7.566 (d, J=7.5 Hz, 2H, C1, C8-phenothiazine), 7.470-7.442 (dd, J=6, 1.5 Hz, 2H, C4, C5-phenothiazine), 7.369-7.236 (m, 4H, C2, C3, C6, C7-phenothiazine), 6.991-6.961 (t, J=7.5 Hz, 1H, C5-phenyl), 6.852-6.835 (d, J=8.5 Hz, 1H, C4-phenyl), 6.798 (s, 1H, C2-phenyl), 6.581-6.565(dd, J=8, 1.5 Hz, 1H, C6-phenyl), 4.178 (s, 2H, methylene-$CH_2$), 3.923 (s, 1H, NH); $^{13}$C-NMR (125 MHz, $CDCl_3$) δ: 169.225 (C=O), 148.411, 142.353, 136.262, 134.907, 131.071, 128.542, 127.009, 126.011, 124.134, 120.490, 116.717, 112.926 (Aromatic carbons), 54.023 (methylene carbon); MS (ESI) *m/z*: 413.1 (M+2, 49%), 412.2 (M+1, 50%); Anal. Calcd for $C_{20}H_{15}BrN_2OS$: C, 58.40; H, 3.68; N, 6.81; Found: C, 58.52; H, 3.64; N, 6.82%.

### 2.12. 2-((4-bromophenyl)amino)-1-(10H-phenothiazin-10-yl)ethan-1-one (9p)

Yield: 55%; MP: 177-189ºC, $^1$H-NMR (500 MHz, $CDCl_3$) δ: 7.593, 7.578 (d, J=7.5 Hz, 2H, C1, C8-phenothiazine), 7.476-7.458 (dd, J=9 Hz, 2H, C4, C5-phenothiazine), 7.372-7.357 (dd, J=7.5, 1.5 Hz, 2H, C3, C5-phenyl), 7.342-7.214 (m, 4H, C2, C3, C6, C7-phenothiazine), 6.571-6.549 (dd, J=11, 1.5 Hz, 2H, C2,C6-phenyl), 4.183 (s, 2H, Methylene $CH_2$ ), 3.551 (s, 1H, NH); $^{13}$C-NMR (125 MHz, $CDCl_3$) δ: 169.331 (C=O), 148.465, 142.341, 136.318, 134.891, 131.127, 128.584, 127.102, 126.018, 124.177, 120.536, 116.520, 112.961 (Aromatic carbons), 54.112 (methylene carbon); MS (ESI) *m/z*: 413.4 (M+2, 49%), 412.3 (M+1, 50%); Anal. Calcd for $C_{20}H_{15}BrN_2OS$: C, 58.40; H, 3.68; N, 6.81; Found: C, 58.51; H, 3.62; N, 6.80%.

### 2.13. 2-((3,5-dichlorophenyl)amino)-1-(10H-phenothiazin-10-yl)ethan-1-one (10p)

Yield: 58%; MP: 185-187ºC, $^1$H-NMR (500 MHz, $CDCl_3$) δ: 7.592, 7.577 (d, J=7.5 Hz, 2H, C1, C8-phenothiazine), 7.471-7.453 (dd, J=9, 1.5 Hz, 2H, C4, C5-phenothiazine), 7.369-7.336 (td, J=7.5, 1.5 Hz, 2H, C2, C7-phenothiazine), 7.282-7.252 (td, J=7.5, 1.5 Hz, 2H, C3, C6-phenothiazine), 6.824 (s, 2H, C2, C6-phenyl), 6.512 (s, 1H, C4-phenyl), 4.183, (s, 2H, methylene-$CH_2$), 3.902, (s, 1H,NH); $^{13}$C-NMR (125 MHz, $CDCl_3$) δ: 170.115 (C=O), 147.863, 142.231, 136.781, 132.315, 130.848, 128.511, 126.456, 123.447, 121.619, 115.021 (Aromatic carbons), 54.724 (methylene carbon); MS (ESI) *m/z*: 405.1 (M+4, 5%), 403.2 (M+2, 32%), 402.1 (M+1, 74%); Anal. Calcd for $C_{20}H_{14}Cl_2N_2OS$: C, 59.86; H, 3.52; N, 6.98; Found: C, 59.91; H, 3.56; N, 6.96%.

### 2.14. 2-((3,5-dibromophenyl)amino)-1-(10H-phenothiazin-10-yl)ethan-1-one (11p)

Yield: 54%; MP: 191-194ºC, $^1$H-NMR (500 MHz, $CDCl_3$) δ: 7.574-7.529 (dd, J=22.5, 8 Hz, 2H, C1, C8-phenothiazine), 7.474-7.432 (dd, J=21, 7.5 Hz, 2H, C4, C5-phenothiazine), 7.369-7.311 (td, J=14, 7.5 Hz, 2H, C2, C7-phenothiazine), 7.282-7.226 (m, 3H, C3, C6-phenothiazine, C4-phenyl), 6.518 (s, 2H, C2, C6-phenyl), 4.178, (s, 2H, methylene-$CH_2$), 3.462, (s, 1H, NH); $^{13}$C-NMR (125 MHz, $CDCl_3$) δ: 170.462 (C=O), 147.281, 142.515, 136.388, 133.407, 130.933, 127.738, 126.102, 123.623, 120.009, 115.648 (Aromatic carbons), 54.852 (methylene carbon); MS (ESI) *m/z*: 494.3 (M+4, 46%), 492.2 (M+2, 97%), 491.4 (M+1, 49%); Anal. Calcd for $C_{20}H_{14}Br_2N_2OS$: C, 49.00; H, 2.88; N, 5.71; Found: C, 49.11; H, 2.92; N, 5.74%.

### 2.15. 2-((3-chloro-4-fluorophenyl)amino)-1-(10H-phenothiazin-10-yl)ethan-1-one (12p)

Yield: 59%; MP: 175-177°C; $^1$H-NMR (500 MHz, $CDCl_3$) δ (ppm); 7.643, 7.628 (d, J=7.5 Hz, 2H, C1, C8-phenothiazine), 7.524, 7.509 (d, J=7.5 Hz, 2H, C4, C5-phenothiazine), 7.438-7.375 (td, J=14, 7.5 Hz, 2H, C2, C7-phenothiazine), 7.291-7.227 (td, J=14, 7.5 Hz, 2H, C3, C6-phenothiazine), 7.105-6.889 (m, 3H, C2, C5, C6-phenyl), 4.261 (s, 2H, methylene-$CH_2$), 3.568 (s, 1H, NH); $^{13}$C-NMR (125 MHz, $CDCl_3$) δ: 167.328 (C=O), 146.438, 142.373, 140.152, 134.651, 130.825, 128.174, 127.079, 126.653, 123.138, 121.647, 120.367, 115.552 (Aromatic carbons), 55.672 (methylene carbon); MS (ESI) *m/z*: 386.5 (M+2, 24%), 385.7 (M+1, 75%); Anal. Calcd for $C_{20}H_{14}ClFN_2OS$:

C, 62.42; H, 3.67; N, 7.28; Found: C, 62.49; H, 3.67; N, 7.31%.

### 2.16. 2-((2-bromo-4-fluorophenyl)amino)-1-(10H-phenothiazin-10-yl)ethan-1-one (13p)

Yield: 56%; MP: 189-191ºC, $^{1}$H-NMR (500 MHz, $CDCl_3$) δ 7.578, 7.561 (d, J=8.5 Hz, 2H, C1, C8-phenothiazine), 7.448-7.430 (dd, J=9, 1.5 Hz, 2H, C4, C5-phenothiazine), 7.345-7.311 (td, J=17, 7.5 Hz, 2H, C2, C7-phenothiazine) 7.255-7.224 (td, J=15.5, 7.5 Hz, 2H, C3, C6-phenothiazine), 7.135 (s, C3-phenyl), 6.821, 6.805 (d, J=8 Hz, 1H, C5-phenyl), 6.512, 6.497, (d, J=7.5 Hz, 1H, C6-phenyl), 4.180 (s, 2H, Methylene $CH_2$), 3.707 (s, 1H, NH); $^{13}$C-NMR (125 MHz, $CDCl_3$) δ: 169.731 (C=O), 146.085, 141.727, 135.325, 132.411, 130.319, 128.324, 127.227, 126.210, 124.463, 122.302, 120.694, 115.049 (Aromatic carbons), 53.522 (methylene carbon); MS (ESI) *m/z*: 431.6 (M+2, 49%), 430.4 (M+1, 50%); Anal. Calcd for $C_{20}H_{14}BrFN_2OS$: C, 55.96; H, 3.29; N, 6.53; Found: C, 56.03; H, 3.35; N, 6.54%.

### 2.17. 2-((3-nitrophenyl)amino)-1-(10H-phenothiazin-10-yl)ethan-1-one (14p)

Yield: 56%; MP: 195-196ºC, $^{1}$H-NMR (500 MHz, $CDCl_3$) δ; 7.669, 7.653 (d, J=8 Hz, 2H, C1, C8-phenothiazine), 7.581-7.562 (dd, J=9.5, 1.5 Hz, 2H, C4, C5-phenothiazine), 7.466-7.432 (td, J=7.5, 1.5 Hz, 2H, C2, C7-phenothiazine), 7.352-7.321 (td, J=6, 1.5 Hz, 2H, C3,C6-phenothiazine), 7.117-7.089, (t, J=7 Hz, 1H, C5-phenyl), 6.737,6.721 (d, J=8 Hz, 1H, C4-phenyl), 6.658 (s, 1H, C2-phenyl), 6.432, 6.415 (d, J= 8.5 Hz, 1H, C6-phenyl), 4.201 (s, 2H, Methylene-$CH_2$), 3.931 (s, 1H, NH); $^{13}$C-NMR (125 MHz, $CDCl_3$) δ: 171.802 (C=O), 148.012, 141.209, 135.218, 134.164, 131.365, 129.432, 127.321, 126.299, 123.627, 120.613, 116.510, 112.388 (Aromatic carbons), 53.258 (methylene carbon); MS (ESI) *m/z*: 378.5 (M+1, 36%); Anal. Calcd for $C_{20}H_{15}N_3O_3S$: C, 63.65; H, 4.01; N, 11.13; Found: C, 63.71; H, 3.98; N, 11.16%.

### 2.18. 2-((4-nitrophenyl)amino)-1-(10H-phenothiazin-10-yl)ethan-1-one (15p)

Yield: 52%; MP: 192-194ºC; $^{1}$H-NMR (500 MHz, $CDCl_3$) δ; 7.652, 7.636 (d, J=8 Hz, 2H, C1, C8-phenothiazine), 7.536, 7.521 (d, J=7.5 Hz, 2H, C4, C5-phenothiazine), 7.440-7.410 (td, J=15, 1.5 Hz, 2H, C2, C7-phenothiazine), 7.552-7.522 (td, J=15, 1.5 Hz, 2H, C3, C6-phenothiazine), 7.202, 7.188 (d, J=7 Hz, 2H, C3, C5-phenyl), 6.638, 6.619 (d, J=9.5 Hz, 2H, C2, C6-phenyl), 4.196 (s, 2H, methylene-$CH_2$) 3.612 (s, 1H, NH); $^{13}$C-NMR (125 MHz, $CDCl_3$) δ: 171.105 (C=O), 146.423, 140.985, 134.751, 132.158, 130.564, 128.271, 126.385, 124.631, 122.169, 116.736 (Aromatic carbons), 53.635 (methylene carbon); MS (ESI) *m/z*: 378.5 (M+1, 28%); Anal. Calcd for $C_{20}H_{15}N_3O_3S$: C, 63.65; H, 4.01; N, 11.13; Found: C, 63.72; H, 4.02; N, 11.14%.

### 2.19. 2-((2-chloro-4-nitrophenyl)amino)-1-(10H-phenothiazin-10-yl)ethan-1-one (16p)

Yield: 56%; MP: 201-205ºC, $^{1}$H-NMR (500 MHz, $CDCl_3$) δ: 8.202 (s, 1H, C3-phenyl), 7.984-7.961 (dd, J=11.5, 2.5 Hz, 1H, C5-phenyl), 7.592, 7.577 (d, J=7.5 Hz, 2H, C1, C8-phenothiazine), 7.473-7.455 (dd, J=7.5, 1.5 Hz, 2H, C4, C5-phenothiazine), 7.371-7.337 (td, J=8, 1.5 Hz, 2H, C2, C7-phenothiazine), 7.285-7.252 (td, J=9, 1.5 Hz, 2H, C3, C6-phenothiazine), 6.728, 6.710 (d, J=9 Hz, 1H, C6-phenyl), 4.832 (s, 1H, NH), 4.189 (s, 2H, Methylene-$CH_2$); $^{13}$C-NMR (125 MHz, $CDCl_3$) δ: 172.463 (C=O), 147.618, 141.241, 136.553, 132.328, 130.432, 128.263, 127.281, 126.642, 124.518, 122.332, 120.174, 116.155 (Aromatic carbons), 54.104 (methylene carbon); MS (ESI) *m/z*: 413.7 (M+2, 25%), 412.6 (M+1, 74%); Anal. Calcd for $C_{20}H_{14}ClN_3O_3S$: C, 58.33; H, 3.43; N, 10.20; Found: C, 58.41; H, 3.48; N, 10.24%.

### 2.20. 2-((4-chloro-2-nitrophenyl)amino)-1-(10H-phenothiazin-10-yl)ethan-1-one (17p)

Yield: 49%; MP: 199-201ºC, $^{1}$H-NMR (500 MHz, $CDCl_3$) δ: 8.112 (s, 1H, C3-phenyl), 7.593, 7.577 (d, J=8 Hz, 2H, C1, C8-phenothiazine), 7.473, 7.459 (d, J=7 Hz, 2H, C4, C5-phenothiazine), 7.372-7.347, (t, J=6 Hz, 2H, C2, C7-phenothiazine), 7.342-7.255 (m, 3H, C3, C6-phenothiazine, C5-phenyl), 6.774, 6.757 (d, J=8.5 Hz, 1H, C6-phenyl), 6.108 (s, 1H, NH), 4.190 (s, 2H, Methylene-$CH_2$); $^{13}$C-NMR (125 MHz, $CDCl_3$) δ: 171.961 (C=O), 147.322, 141.752, 137.025, 132.331, 130.584, 128.626, 127.811, 126.426, 124.733, 122.501, 120.227, 116.513 (Aromatic carbons), 54.039 (methylene carbon); ESI-MS *m/z*: 413.2 (M+2, 25%), 412.5 (M+1, 75%); Anal. Calcd for $C_{20}H_{14}ClN_3O_3S$: C, 58.33; H, 3.43; N, 10.20; Found: C, 58.38; H, 3.46; N, 10.22%.

### 2.21. 2-((2-oxo-2-(10H-phenothiazin-10-yl)ethyl)amino) benzoic acid (18p)

Yield: 45%; MP: 165-167ºC; $^{1}$H-NMR (500 MHz, $CDCl_3$) δ; 12.283 (s, 1H, OH), 7.837, 7.821 (d, J=8 Hz, 1H, C3-phenyl), 7.622, 7.606 (d, J=8 Hz, 2H, C1, C8-phenothiazine), 7.531-7.516 (d, J=7.5 Hz, 2H, C4, C5-phenothiazine), 7.441-7.426 (td, J=7.5, 1.5 Hz, 2H, C2, C7-phenothiazine), 7.355-7.340 (td, J=7.5, 1.5 Hz, 2H, C3, C6-phenothiazine), 7.244-7.218 (t, J=6.5 Hz, 1H, C5-phenyl), 7.001 -6.918 (m, 2H, C4, C6-phenyl), 4.246 (s, 2H, methylene-$CH_2$) 3.935 (1H, NH); $^{13}$C-NMR (125 MHz, $CDCl_3$) δ: 184.128 (COOH), 170.132 (C=O), 146.626, 141.427, 135.628, 132.521, 130.629, 128.238, 127.442, 126.164, 123.426, 121.621, 119.895, 115.926 (Aromatic carbons), 53.811 (methylene carbon); MS (ESI) *m/z*: 377.9 (M+1, 38%); Anal. Calcd for $C_{21}H_{16}N_2O_3S$: C, 67.01; H, 4.28; N, 7.44; Found: C, 67.10; H, 4.31; N, 7.47%.

### 2.22. 2-(4-(4-chlorophenyl)piperazin-1-yl)-1-(10H-phenothiazin-10-yl)ethan-1-one (19p)

Yield: 85%; MP: 177-180ºC; $^{1}$H-NMR (500 MHz, $CDCl_3$) δ; 7.671, 7.655 (d, J=8 Hz, 2H, C1, C8-phenothiazine), 7.518, 7.503 (d, J=7.5 Hz, 2H, C4, C5-phenothiazine), 7.434-7.403 (td, J=15.5, 1.5 Hz, 2H, C2, C7-phenothiazine), 7.253-7.220 (td, J=15, 1.5 Hz, 2H, C3, C6-phenothiazine), 7.121, 7.108 (d, J=6.5 Hz, 2H, C3, C5-phenyl), 6.631, 6.613 (d, J=9 Hz, 2H, C2, C6-phenyl), 4.135 (s, 2H, methylene-$CH_2$) 3.212-3.188 (m, 4H, piperazine); 2.712-2.689 (m, 4H, piperazine); $^{13}$C-NMR (125 MHz,

$CDCl_3$) δ: 169.731 (C=O), 145.549, 139.438, 134.726, 131.461, 129.612, 127.742, 126.514, 125.843, 122.472, 115.857 (Aromatic carbons), 53.948 (methylene carbon); 52.482, 50.791 (piperazine carbons); MS (ESI) *m/z*: 437.6 (M+2, 25%), 436.3 (M+1, 74%); Anal. Calcd for $C_{24}H_{22}ClN_3OS$: C, 66.12; H, 5.09; N, 9.64; Found: C, 66.19; H, 5.15; N, 9.67%.

### 2.23. 2-(4-(4-nitrophenyl)piperazin-1-yl)-1-(10H-phenothiazin-10-yl)ethan-1-one (20p)

Yield: 77%; MP: 181-182ºC; $^1$H-NMR (500 MHz, $CDCl_3$) δ; 7.690, 7.674 (d, J=8 Hz, 2H, C1, C8-phenothiazine), 7.527, 7.510 (d, J=8.5 Hz, 2H, C4, C5-phenothiazine), 7.421-7.389 (td, J=16, 1.5 Hz, 2H, C2, C7-phenothiazine), 7.234-7.204 (td, J=15, 1.5 Hz, 2H, C3, C6-phenothiazine), 7.160, 7.146 (d, J=7 Hz, 2H, C3, C5-phenyl), 6.625, 6.607 (d, J=9 Hz, 2H, C2, C6-phenyl), 4. 182 (s, 2H, methylene-$CH_2$) 3.225-3.201 (m, 4H, piperazine); 2.715-2.692 (m, 4H, piperazine); $^{13}$C-NMR (125 MHz, $CDCl_3$) δ: 169.769 (C=O), 146.128, 140.432, 135.583, 131.728, 129.835, 127.934, 126.623, 125.782, 122.681, 116.125 (Aromatic carbons), 54.263 (methylene carbon); 53.573, 51.382 (piperazine carbons); MS (ESI) *m/z*: 447.71 (M+1, 42%); Anal. Calcd for $C_{24}H_{22}N_4O_3S$: C, 64.56; H, 4.97; N, 12.55; Found: C, 64.65; H, 5.02; N, 12.57%.

## 3. ANTITUBERCULAR SCREENING

The synthesized compounds were screened against *M. tuberculosis* (H37Rv) using Microplate Alamar Blue Assay (MABA) [18, 19]. The outer perimeter wells of sterile 96 wells plate were added with 200µL of sterile deionized water to avoid evaporation of the medium during incubation. 100 µL of Middlebrook 7H9 broth was added to the test wells, followed by addition of the test compounds at concentrations ranging from 100 to 0.2µg/mL. Later, the plates were sealed with parafilm and incubated at 37ºC for five days. After incubation, each test well was added with 25µL of 1:1 mixture of Alamar blue reagent and 10% tween 80, and the incubation was continued for another 24 hours. The pink color developed in the wells was recorded as growth, while the blue color was recorded as the absence of bacterial growth. The lowest concentration of the compounds that prevented the color change from blue to pink was defined as the minimum inhibitory concentration (MIC). All determinations were done in triplicate.

## 4. ANTIBACTERIAL SCREENING

The synthesized compounds were further evaluated for their antibacterial activity against *Staphylococcus aureus* (ATCC 25323) and *Escherichia coli* (ATCC 35218) by agar plate disc diffusion method [18, 20]. The agar plates were first prepared by spreading 20 mL of Mueller Hinton Agar (MHA, Hi- Media) on petri plates and were allowed to solidify. Then, a 24/48 hold culture of selected bacteria was mixed with sterile physiological saline (0.85%), and the turbidity was adjusted to standard inoculum of Mac- Farland scale 0.5 [~$10^6$ Colony Forming Units (CFU) per mL]. The obtained inoculum was spread over the surface of the solidified media. The paper discs (Whatman no.1) of 6 mm diameter were impregnated with test compounds at 20µL per disc and were placed over the media that was already inoculated with different bacterial strains. Ciprofloxacin (5µg/disc, Hi-Media) was used as a positive control and Dimethylsulfoxide (DMSO) was used as a negative control. Plates were then incubated for 24 hours at 37°C. The lowest concentration that completely inhibits visible growth is defined as MIC [21] and all the determinations were done in triplicates.

## 5. BBB PERMEABILITY (PAMPA ASSAY)

The 96-well acceptor plate was hydrated with a buffer of pH 7.4 for 12 hrs and their wells were coated with 5µL of 20mg/ml PBL in dodecane. They were filled with 200 µL of buffer of pH 7.4. A solution containing 5mg of drug was prepared in 1mL of DMSO. 10 µL of the solution was further diluted to 200-fold with the buffer to get the final concentration of 25µg/ml. 200µL of the solution was added to the wells of the donor plate. The acceptor and donor plates were then sandwiched and left undisturbed for 18 hrs. The concentration of drugs in both acceptor and donor plates was determined by measuring the absorbance at their corresponding wavelengths using the microplate reader [18, 21]. Effective permeability (Pe) of the compounds was calculated as follows,

$$Pe\ (cm/s) = \{-\ln[1-CA(t)/Ceq]\}/[A*(1/VD+1/VA)*t]$$

Pe = permeability in cm per second

A = filter area (0.3 $cm^2$)

VD = donor well volume (0.3 ml)

VA = acceptor well volume (0.2 ml)

t = incubation time (seconds)

CA(t) = concentration in acceptor well at time t

CD(t) = concentration in donor well at time t

$$Ceq = [CD(t)*VD + CA(t)*VA]/(VD+VA)$$

The compounds were further classified as follows based on the nature of BBB permeability

CNS+= high BBB permeation=Pe ($10^{-6}$ cm $s^{-1}$) >4.0

CNS- =low BBB permeation=Pe ($10^{-6}$ cm $s^{-1}$) <2.0

CNS+/-=BBB permeation uncertain=Pe ($10^{-6}$ cm $s^{-1}$) from 4.0 to 2.0

## 6. *IN-VITRO* CYTOTOXICITY SCREENING

Cytotoxicity of the synthesized compounds was determined by MTT assay using Kidney epithelial VERO cells [22, 23]. The cells were seeded at $10^5$ cells/ well in 100µl of the Eagle's Minimum Essential Medium (EMEM) and incubated for 24 hours at 37°C in 5% $CO_2$ atmosphere. The cells were treated with test compounds of varying concentrations ranging from 7.8125 to 1000 µg/mL and incubated for another 72 hours. An equal volume (20 µL/well) of 0.5% solution of 3-(4,5-dimethyl-2-thiazolyl)-2,5-diphenyl-tetrazolium bromide (MTT) in phosphate buffered saline was added to each well and incubated for 4 hours. 1 mL of DMSO was then added to the wells and absorbance was measured at 570 nm using microplate reader to determine the cell viability. The percentage growth of the cells was calculated for each well relative to the control and the concentration required for 50%

inhibition of the viable cells ($CC_{50}$) was determined graphically [22, 23]. Percentage cell viability was calculated by using the following formula:

Percentage cell viability= Absorption of test/ absorption of control x 100

## 7. MOLECULAR PROPERTY & TOXICITY PREDICTION

The toxicity and drug-relevant properties (cLogP, cLogS, hydrogen bond donor, hydrogen bond acceptor, and drug-likeness) were determined using OSIRIS DataWarrior [24]. Polar surface area and lipophilicity are the two important properties of a molecule for its transport across biological membranes. The higher the Total Polar Surface Area (TPSA), the poor the bioavailability and absorption of the drug. Percentage absorption (%ABS) was calculated using the following formula,

Percentage of absorbance = 109-(0.345 × TPSA).

## 8. HOMOLOGY MODELING

Three-dimensional structure of Type-2 NADH dehydrogenase (ndh-2) of the *Mycobacterium tuberculosis (strain CDC 1551)* was constructed by homology modeling using ModFOLD version 6.0 web server [25-27]. The sequence of the ndh-2 was retrieved from UniProt server. The model was validated using the RAMPAGE [28], PROCHECK [29], ERRAT [30], Verify 3D [31], and Global model quality score. Visualization of the model was done with Chimera. The Model was refined using Dockprep and PDB2PQR utility [32].

## 9. MOLECULAR DOCKING

### 9.1. Protein Preparation

The protein structure of Mtb ndh-2 developed through homology modeling was used for the purpose of molecular docking. The protein structure was preprocessed in order to be used as a receptor for docking. The missing side chain residues were assessed to confirm the integrity of the protein structure. Then, the protein was subjected to energy minimization using OPLS-2005 force field.

### 9.2. Grid Generation

Molecular docking cannot be done until the receptor grids are generated since the protein is large and cannot be used as such. The shape and properties of the receptor are represented in the grid by applying different sets of fields on the lattice points. The residues forming the quinone binding motif was assigned as the centroid of the grid and then the size was confined to 10Å.

### 9.3. Ligand Preparation

2D structures of the ligands were drawn and converted to 3D structures. The ligands were prepared by applying the OPLS-2005 force field. All the possible protonation and ionization states of the ligands were computed at pH 7.4. Tautomers were then generated for chemical groups in the molecule and the number of stereoisomers was limited to 32 per ligand.

### 9.4. Ligand Docking

The prepared ligands were flexibly docked into the rigid protein structure of Mtb ndh-2 through extra precision (XP) mode. Thereby, the ligand poses were examined and weeded out the false positives for better correlation between good poses and the good score.

## 10. RESULTS AND DISCUSSION

### 10.1. Off-target Virtual Screening and Filtering of Designed Molecules

The design strategy was a structural modification of neuroleptic phenothiazine drug Chlorpromazine (CPZ), for improved antitubercular activity. The molecules were designed using CPZ as a template. Hence, the designed molecules were virtually screened against dopamine D2 (PDB: 6CM4) and D3 (PDB: 3PBL) receptors through high-throughput virtual screening module of Schrodinger [17]. Later, we filtered the molecules with a cut-off of docking score ≤ 2.0 Kcal/mol. The filtered molecules produced least interactions with dopamine receptors (D2 & D3), hence may produce no/ less unwanted antipsychotic side effect. We obtained a total of 20 hit molecules out of 130 designed molecules, having the least interaction with dopamine receptors. Risperidone, the co-crystallized ligand and CPZ, the template molecule produced docking score of -9.0963 and 7.9910 Kcal/mol respectively, against D2 receptor (Fig. **2**). Risperidone and CPZ produced the essential interaction with ASP114, while such interaction was missing with the hits. Docking pose of a hit obtained from off-target virtual screening and filtering against D2 receptor is depicted in Fig. (**2**). Eticlopride, the co-crystallized ligand and CPZ produced docking score of -8.6115 and -8.6093 Kcal/mol respectively, against D3 receptor (Fig. **3**). Eticlopride and CPZ produced essential interaction with ASP110, while this was missing in the hits obtained. Docking pose of a hit obtained from this off-target virtual screening and filtering against D3 receptor is depicted in Fig. (**3**).

### 10.2. Chemistry

All the designed molecules were synthesized as shown in Scheme **1** *i.e.* synthesis of phenothiazine **(b)** followed by 2-chloro-1-(10H-phenothiazin-10-yl)ethan-1-one **(1p)**. Later, the final derivatives were synthesized on reaction of **1p** with different phenyl amines/phenylpiperazines. The progress of reactions was monitored by thin layer chromatography and column chromatography was performed to obtain pure novel phenothiazine derivatives. The yield was in the range of 45 to 95 percent. Purity of the compounds was ascertained by melting point and elemental analysis. The assigned structures were then confirmed through spectral analyses *viz*. $^{1}H$ and $^{13}C$ NMR spectroscopy and Mass spectrometry.

### 10.3. Antitubercular Activity

All the synthesized compounds were screened against Mtb (H37Rv) by using Micro-plate Alamar Blue assay (MABA) [19] and the results were presented in Table **1**. Structure-activity relationship (SAR) was established from the results of antitubercular screening. The nitro compounds were found to be more active among all the derivatives. Fur-

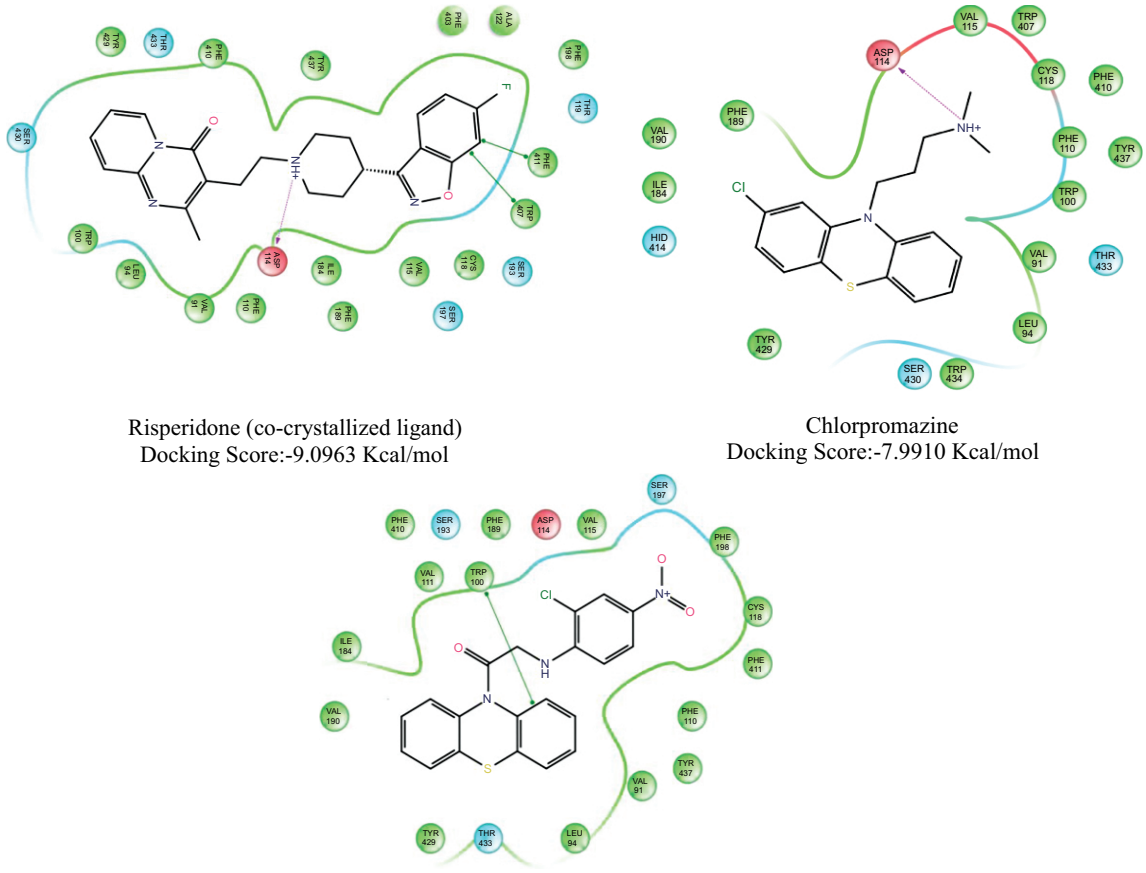

Risperidone (co-crystallized ligand)
Docking Score:-9.0963 Kcal/mol

Chlorpromazine
Docking Score:-7.9910 Kcal/mol

Molecule 16p
Docking score:-1.8519 Kcal/mol

**Fig. (2).** Docking poses of risperidone, chlorpromazine and a designed molecule against D2 receptor (PDB: 6CM4).

ther, the meta and para substituted nitro compounds **(14p, 15p, 16p)** showed better activity (1.56 µg/ml) in comparison to ortho substituted compound **(17p)** (3.13 µg/ml). The meta-substituted halogen compounds (**10p-12p)** were found to show better activity in comparison to ortho/ para substituted halogen compound **(13p)**. The number of halogen substitution seems to play a significant role, as the di-substituted halogen compounds **(10p to 13p)** produced better activity than monosubstituted compounds. The electron withdrawing nature of halogen and nitro group also seems to be important for the activity of the compounds. In compounds **19p** and **20p**, the acyl linker was replaced with piperazinyl linker, leading to a reduction in the activity. Further, the compound with nitro substitution at para position (**19p)** was found more active in comparison to chloro substitution (**20p)**. It indicated that the piperazinyl linker might not have many roles in improving the activity.

### 10.4. Antibacterial Activity

The compounds were also screened for antibacterial activity by disc diffusion method [20]. The compounds **(14p, 15p, 16p)** displayed maximum inhibition against *S. aureus* and *E. coli* at MIC of 0.98µg/ml and 3.91µg/ml, respectively (Table **1**). The activity was better against *S. aureus* in comparison to *E. coli* and Mtb. The nitro substituted compounds **(14p, 15p, 16p)** were more active in comparison to halogen substituted compounds **(3p to 13p)** and also the para- and meta-substitution was found essential to produce the activity.

### 10.5. BBB Permeability

BBB permeability determines the possible CNS effect of the compounds and all the designed phenothiazine derivatives were screened for BBB permeability by Parallel artificial membrane permeability assay (PAMPA). The permeability of the compounds was compared with commercial drugs and classified as high permeable (CNS+), low permeable (CNS-) and permeable uncertain (CNS+/-). The chlorpromazine and diazepam produced effective permeability (Pe) of $6.1 \times 10^{-6}$ and $12.4 \times 10^{-6}$ cm/s respectively and were classified as high permeable drugs, whereas, atenolol, verapamil and levofloxacin produced effective permeability of $1.1 \times 10^{-6}$, 0.0 and 0.0 cm/s respectively and classified as low permeable drugs. The effective permeability (Pe) of the screened compounds (**1p to 18p**) was found in the range of $2.8 \times 10^{-6}$ to $3.8 \times 10^{-6}$ cm/s and were classified as permeability uncertain. The compounds **19p** and **20p** produced effective permeability (Pe) of $4.5 \times 10^{-6}$ and $4.2 \times 10^{-6}$ cm/s respectively and were classified as permeability high (Table **2**). The reduced BBB permeability could reduce the CNS effect of the developed compounds (**1p to 18p**) in comparison to chlorpromazine.

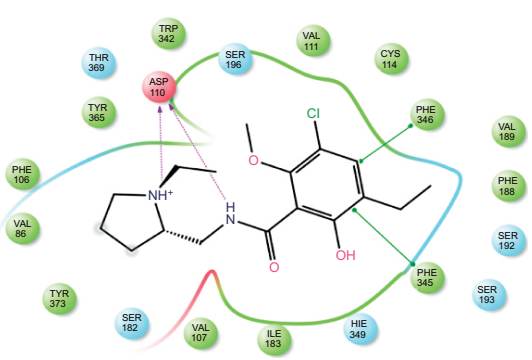


Eticlopride
Docking score:- 8.6115 Kcal/mol

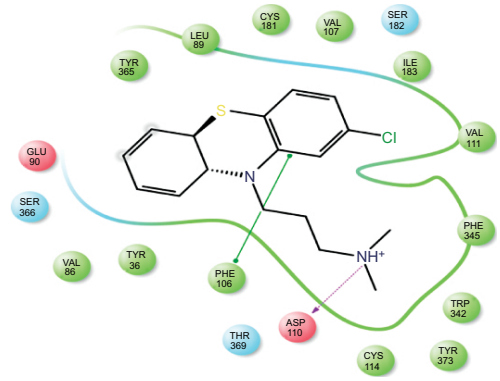


Chlorpromazine
Docking score:- 8.6093 Kcal/mol

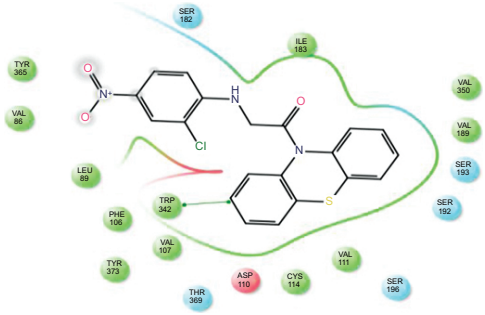


Molecule 16p
Docking score:-1.3852 Kcal/mol

**Fig. (3).** Docking poses of eticlopride, chlorpromazine and a designed molecule against D3 receptor (PDB: 3PBL).

### 10.6. Cytotoxicity Screening (VERO cells) and Selectivity Index

The antimicrobial drugs should be free from toxicity towards normal mammalian cells. Therefore, all the compounds were screened against VERO (monkey kidney epithelial) cells to evaluate their toxicity. The concentration required to produce 50% inhibition ($CC_{50}$) was determined and was found in the range of 84.71 to 201.82 µg/mL (Table **3**). All the compounds were found to be non-toxic to mammalian cells. The selectivity of drug molecules towards a desired activity is a challenging task in drug discovery. The compounds should be toxic only towards Mtb and other microbial species rather than the normal human cells. The selectivity index (SI) was calculated from the obtained mammalian cell cytotoxicity ($CC_{50}$) and tubercular cytotoxicity (MIC). The potent compounds (**14p, 15p & 16p**) from antitubercular screening showed SI more than 57, indicating their selectivity towards Mtb rather against normal human cells.

### 10.7. Molecular Property and Toxicity Prediction

The reduced bioavailability on oral administration and the associated toxicity are the prime factors for the failure of drug candidates in clinical development stage. About one-third of drug candidates fail due to their poor pharmacokinetic profiles. Hence, computational study was performed to predict the molecular property and toxicity of the developed compounds [14]. Lipophilicity defines the pharmacokinetics and also pharmacodynamics of a drug molecule. It was determined by calculating clogP using OSIRIS DataWarrior and was found in the range between 2.92 and 5.93. The clogP of the potent compounds (**14p, 15p & 16p**) was found to be 3.71, 3.41 and 4.32, respectively. Topological Polar Surface Area (TPSA) was computed and was found to be 57.64 for compounds **2p** to **13p**, and 103.46 for compounds **14p** to **17p**, while 94.94, 52.09 and 97.91 for the compounds **18p**, **19p** and **20p,** respectively. The good percentage of drug absorbance could lead to better oral bioavailability. Hence, the percentage absorption was calculated and was found to be over 73 percent for all the compounds. Molecular descriptors like hydrogen bond donor, hydrogen bond acceptor and drug likeness were computed and were found within the desired range. The results of the study are presented in Table **4**.

The fragments of a given molecule are the indicators of toxicity risk. Therefore, all the molecules were predicted for mutagenicity, tumorigenicity, and irritancy through OSIRIS DataWarrior. Except **1p**, none of the molecules in the study were predicted to be mutagenic and tumorigenic but irritancy was noticed. Molecules **10p** and **16p** were indicated with low levels of irritancy and molecules **1p**, **19p** and **20p** were indicated with high level of irritancy (Table **4**). The developed compounds were devoid of major toxicity risks and further development of these phenothiazine classes of compounds might be fruitful.

**Table 1. Antitubercular and antibacterial activity of the synthesized compounds.**

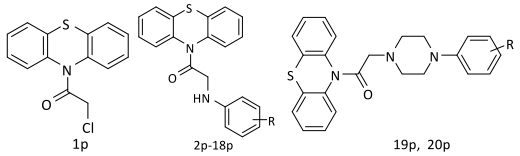


| Code | R | MIC in µg/mL (µM) [a] | MIC in µg/mL (µM) [b] | MIC in µg/mL (µM) [c] |
|---|---|---|---|---|
| 1p | - | 62.50 (226.65) | 62.50 (226.65) | 50 (181.32) |
| 2p | H | 15.63 (47.01) | 31.25 (94.00) | 25 (75.20) |
| 3p | 2-Cl | 15.63 (46.39) | 31.25 (92.76) | 25 (74.21) |
| 4p | 3-Cl | 7.81 (23.18) | 31.25 (92.76) | 12.5 (37.10) |
| 5p | 4-Cl | 7.81 (23.18) | 31.25 (92.76) | 12.5 (37.10) |
| 6p | 3-F | 7.81 (22.28) | 31.25 (89.18) | 12.5 (35.67) |
| 7p | 4-F | 7.81 (22.28) | 31.25 (89.18) | 12.5 (35.67) |
| 8p | 3-Br | 7.81 (18.98) | 31.25 (75.97) | 12.5 (30.38) |
| 9p | 4-Br | 7.81 (18.98) | 31.25 (75.97) | 12.5 (30.38) |
| 10p | 3,5-diCl | 3.91 (9.74) | 7.81 (19.46) | 6.25 (15.57) |
| 11p | 3,5-diBr | 3.91 (7.97) | 7.81 (15.93) | 6.25 (12.74) |
| 12p | 3-Cl,4-F | 3.91 (10.15) | 7.81 (20.29) | 6.25 (16.24) |
| 13p | 2-Br,4-F | 3.91 (9.10) | 15.63 (36.40) | 6.25 (14.55) |
| 14p | 3-$NO_2$ | 0.98 (2.59) | 3.91 (10.35) | 1.56 (4.13) |
| 15p | 4-$NO_2$ | 0.98 (2.59) | 3.91 (10.35) | 1.56 (4.13) |
| 16p | 2-Cl,4-$NO_2$ | 0.98 (2.37) | 3.91 (9.49) | 1.56 (3.78) |
| 17p | 2-$NO_2$,4-Cl | 1.96 (4.75) | 15.63 (37.94) | 3.13 (7.59) |
| 18p | 2-COOH | 7.81 (20.74) | 15.63 (41.52) | 12.5 (33.20) |
| 19p | 4-Cl | 7.81 (17.91) | 15.63 (35.85) | 12.5 (28.67) |
| 20p | 4-$NO_2$ | 3.91 (8.75) | 7.81 (17.49) | 3.13 (7.00) |
| Chlorpromazine | - | 7.81 (24.49) | 15.63 (49.01) | 12.5 (39.20) |
| Ciprofloxacin | - | 1.95 (5.88) | 3.91 (11.80) | 3.13 (9.44) |
| Pyrazinamide | - | - | - | 3.13 (25.42) |

[a] Minimum Inhibitory Concentration (MIC) against *Staphylococcus aureus* (ATCC 25323);
[b] Minimum Inhibitory Concentration (MIC) against *Escherichia coli* (ATCC35218);
[c] Minimum Inhibitory Concentration (MIC) against *M. tuberculosis* H37Rv.

**Table 2. BBB permeability of commercial drugs and phenothiazine derivatives.**

| Compound Code | $P_e$ x$10^{-6}$ cm/s | Classification |
|---|---|---|
| Chlorpromazine | 6.1±0.059 | CNS+ |
| Atenolol | 1.1±0.021 | CNS- |
| Verapamil | 0.0 | CNS- |
| Diazepam | 12.4±0.263 | CNS+ |
| Levofloxacin | 0.0 | CNS- |
| 1p | 2.8±0.038 | CNS+/- |
| 2p | 3.0±0.041 | CNS+/- |
| 3p | 3.2±0.167 | CNS+/- |

**(Table 2) Contd…**

| Compound Code | $P_e$ x$10^{-6}$ cm/s | Classification |
|---|---|---|
| 4p | 3.3±0.062 | CNS+/- |
| 5p | 3.2±0.251 | CNS+/- |
| 6p | 3.0±0.040 | CNS+/- |
| 7p | 3.0±0.174 | CNS+/- |
| 8p | 3.5±0.262 | CNS+/- |
| 9p | 3.5±0.386 | CNS+/- |
| 10p | 3.6±0.158 | CNS+/- |
| 11p | 3.8±0.053 | CNS+/- |
| 12p | 3.6±0.326 | CNS+/- |
| 13p | 3.8±0.213 | CNS+/- |
| 14p | 3.4±0.091 | CNS+/- |
| 15p | 3.4±0.023 | CNS+/- |
| 16p | 3.7±0.291 | CNS+/- |
| 17p | 3.7±0.082 | CNS+/- |
| 18p | 3.2±0.109 | CNS+/- |
| 19p | 4.5±0.080 | CNS+ |
| 20p | 4.2±0.315 | CNS+ |

CNS+ = high BBB permeation compounds, *i.e.* Pe= > 4.0 * $10^{-6}$ cm $s^{-1}$)
CNS- =low BBB permeation compounds, *i.e.* Pe= < 2.0 * $10^{-6}$ cm $s^{-1}$
CNS+/- =BBB permeation uncertain compounds, *i.e.* Pe =4.0 - 2.0 *$10^{-6}$ cm $s^{-1}$

**Table 3. Cytotoxicity study of phenothiazine derivatives against Kidney epithelial cell (VERO).**

| Compound Code | $CC_{50}$ (µg/ml) [a] | Selectivity Index [b] |
|---|---|---|
| 1p | 201.82±2.476 | 4.0 |
| 2p | 164.35±2.891 | 6.6 |
| 3p | 166.91±9.739 | 6.7 |
| 4p | 154.43±1.924 | 12.3 |
| 5p | 155.07±1.563 | 12.4 |
| 6p | 160.97±10.615 | 12.9 |
| 7p | 157.52±6.291 | 12.6 |
| 8p | 153.28±10.860 | 12.3 |
| 9p | 124.75±2.132 | 10.0 |
| 10p | 129.20±2.728 | 20.7 |
| 11p | 117.64±4.945 | 18.8 |
| 12p | 120.12±2.974 | 19.2 |
| 13p | 115.85±1.846 | 18.5 |
| 14p | 95.91±1.663 | 61.47 |
| 15p | 90.18±2.781 | 57.8 |
| 16p | 97.34±5.126 | 62.4 |
| 17p | 92.76±5.370 | 29.6 |
| 18p | 108.94±4.212 | 8.7 |
| 19p | 89.52±2.618 | 7.1 |
| 20p | 84.71±1.331 | 27.0 |

[a] Data are expressed as mean ± SEM (n =3).
[b] Selectivity index is ratio of cytotoxicity ($CC_{50}$) to *Mtb* MIC.

**Table 4. Molecular properties and predicted toxicity of the synthesized compounds.**

| Code | cLogP | cLogS | HBA | HBD | TSA | TPSA | DL | MU | TU | IR | SI | MF | MC | EA | RB | NR | AR | SA | PA |
|---|---|---|---|---|---|---|---|---|---|---|---|---|---|---|---|---|---|---|---|
| 1p | 4.13 | -5.05 | 2 | 0 | 211 | 45.61 | 1.63 | H | H | H | 0.44 | 0.37 | 0.76 | 4 | 1 | 3 | 2 | 6 | 93.3 |
| 2p | 4.63 | -5.64 | 3 | 1 | 278 | 57.64 | 2.61 | N | N | N | 0.5 | 0.46 | 0.84 | 4 | 3 | 4 | 3 | 8 | 89.1 |
| 3p | 5.24 | -6.38 | 3 | 1 | 293 | 57.64 | 2.65 | N | N | N | 0.48 | 0.45 | 0.79 | 5 | 3 | 4 | 3 | 6 | 89.1 |
| 4p | 5.24 | -6.38 | 3 | 1 | 288 | 57.64 | 2.65 | N | N | N | 0.48 | 0.48 | 0.79 | 5 | 3 | 4 | 3 | 6 | 89.1 |
| 5p | 5.24 | -6.38 | 3 | 1 | 280 | 57.64 | 2.65 | N | N | N | 0.52 | 0.48 | 0.79 | 5 | 3 | 4 | 3 | 8 | 89.1 |
| 6p | 4.73 | -5.96 | 3 | 1 | 267 | 57.64 | 1.27 | N | N | N | 0.48 | 0.46 | 0.84 | 5 | 3 | 4 | 3 | 6 | 89.1 |
| 7p | 4.73 | -5.96 | 3 | 1 | 266 | 57.64 | 1.27 | N | N | N | 0.52 | 0.46 | 0.84 | 5 | 3 | 4 | 3 | 8 | 89.1 |
| 8p | 5.36 | -6.48 | 3 | 1 | 285 | 57.64 | 0.82 | N | N | N | 0.48 | 0.48 | 0.79 | 5 | 3 | 4 | 3 | 6 | 89.1 |
| 9p | 5.36 | -6.48 | 3 | 1 | 295 | 57.64 | 0.82 | N | N | N | 0.52 | 0.48 | 0.79 | 5 | 3 | 4 | 3 | 8 | 89.1 |
| 10p | 5.85 | -7.11 | 3 | 1 | 305 | 57.64 | 2.65 | N | N | L | 0.46 | 0.48 | 0.80 | 6 | 3 | 4 | 3 | 9 | 89.1 |
| 11p | 5.93 | -7.31 | 3 | 1 | 309 | 57.64 | 0.82 | N | N | N | 0.46 | 0.48 | 0.80 | 6 | 3 | 4 | 3 | 9 | 89.1 |
| 12p | 5.34 | -6.69 | 3 | 1 | 289 | 57.64 | 1.31 | N | N | N | 0.50 | 0.48 | 0.80 | 6 | 3 | 4 | 3 | 6 | 89.1 |
| 13p | 5.46 | -6.79 | 3 | 1 | 289 | 57.64 | -0.51 | N | N | N | 0.5 | 0.45 | 0.81 | 6 | 3 | 4 | 3 | 6 | 89.1 |
| 14p | 3.71 | -6.10 | 6 | 1 | 292 | 103.46 | -2.51 | N | N | N | 0.48 | 0.48 | 0.85 | 7 | 4 | 4 | 3 | 6 | 73.3 |
| 15p | 3.71 | -6.10 | 6 | 1 | 292 | 103.46 | -2.51 | N | N | N | 0.51 | 0.48 | 0.85 | 7 | 4 | 4 | 3 | 8 | 73.3 |
| 16p | 4.32 | -6.84 | 6 | 1 | 304 | 103.46 | -2.45 | N | N | L | 0.50 | 0.47 | 0.83 | 8 | 4 | 4 | 3 | 6 | 73.3 |
| 17p | 4.32 | -6.84 | 6 | 1 | 317 | 103.46 | -2.45 | N | N | N | 0.46 | 0.48 | 0.83 | 8 | 4 | 4 | 3 | 6 | 73.3 |
| 18p | 4.12 | -5.65 | 5 | 2 | 286 | 94.94 | 2.47 | N | N | N | 0.44 | 0.46 | 0.86 | 6 | 4 | 4 | 3 | 6 | 73.3 |
| 19p | 5.37 | -5.92 | 4 | 0 | 335 | 52.09 | 6.5 | N | N | H | 0.53 | 0.48 | 0.81 | 6 | 3 | 5 | 3 | 10 | 91.0 |
| 20p | 2.92 | -5.65 | 7 | 0 | 347 | 97.91 | 1.41 | N | N | H | 0.53 | 0.48 | 0.87 | 8 | 4 | 5 | 3 | 10 | 75.2 |

HBA= H-Acceptors; HBD= H-Donor; TSA=Total surface area; TPSA= Total Polar surface area; DL= Druglikeness; MU=Mutagenic; TU=Tumorigenic; IR=Irritant; SI=Shape Index; MF=Molecular Flexibility; MC=Molecular Complexity; EA=Electronegative Atoms; RB=Rotatable Bonds; AR=Aromatic Rings; SA=Symmetric atoms; NR=No. of Rings; PA= Percentage of absorbance; N=none; H=High; L=low.

### 10.8. Homology Modeling

Phenothiazines act by inhibiting Type-2 NADH dehydrogenase (ndh-2), which has a catalytic role in oxidation of NADH to NAD+ with concomitant reduction of quinone to quinol, involved in the energy metabolism for production of ATP. The 3D protein structure of Mtb ndh-2 is not available, therefore, we developed a 3D protein structure/model through homology modeling, using the deposited protein sequence of Mtb ndh-2 *(strain CDC 1551)* available in uniport database [27].

Homology modeling was performed using ModFOLD, version 6.0 web server. The stereochemical property of the developed model was validated using RAMPAGE and PROCHECK servers and the model was found to have more than 90% of residues in the most favoured region (Table **5**).

VERIFY_3D score of the model showed that 87.97% of residues have an average 3D-1D score ≥ 0.2, which is above the cutoff limit of 80%. The overall quality factor was determined by ERRAT and was found to be 82.24%, indicating good quality-resolution of the structure (2.5-4 Å).

The global model quality score was found to be 0.5948, which is greater than 0.4, indicating the model is more complete and confident. It is also indicative that the model is more similar to the native structure. The p-value of the model was $1.434x10^{-6}$, hence there is only 0.0001 % chance of the model becoming wrong.

**Table 5. Ramachandran quality parameter check for the developed homology model of Mtb ndh-2 using RAMPAGE and PROCHECK.**

| Model | Package | Ramachandran Plot Quality (%) | | |
|---|---|---|---|---|
| | | Favored | Allowed | Outlier |
| Mtb ndh-2 | RAMPAGE | 92.2 | 5.3 | 2.5 |
| | PROCHECK | 88.3 | 10.3 | 1.5 |

### 10.9. Superimposition of Protein Structures

The developed protein model of Mtb ndh-2 was superimposed against the known protein structures of *S. aureus* ndh-2 (PDB code:4xdb) and *C. thermarum* ndh-2 (PDB code:4nwz) to check the similarity with the native structures (Fig. **4**). The quinone binding site is the critical part of the model so we calculated Root Mean Square Deviation (RMSD) for the residues forming the quinone binding motif and was found to be ≤0.558 and ≤0.151 against *C. thermarum* and *S. aureus* ndh-2, respectively (Table **6** and

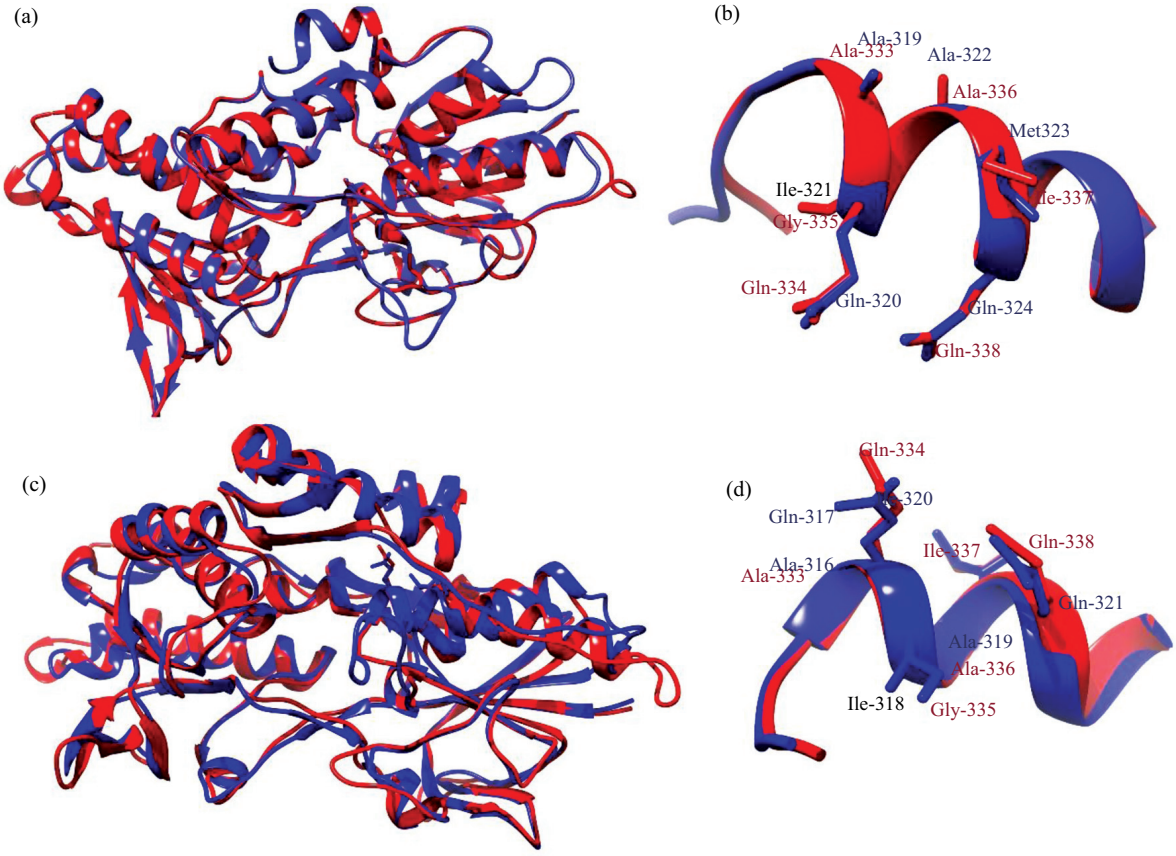


**Fig. (4).** Superimposition of complete protein (**a**) and active motif (**b**) of *S. aureus* ndh-2 (4XDB) over the Mtb ndh-2 model developed through homology modeling. Followed by, superimposition of complete protein (**c**) and active motif (**d**) of *C. thermarum* ndh-2 (4NWZ) over the Mtb ndh-2 model.

**7**). The RMSD value was very low, which indicated that the quinone binding motif of mtb ndh-2 was highly conserved. Thereby, the model can be used for docking analysis to predict the active binding of the inhibitors.

**Table 6. Superimposition of the developed homology model against the protein structure of *S. aureus* ndh-2.**

| Type-2 Quinone Oxidoreductase (ndh-2) of *S. aureus* (PDB Code: 4XDB) | Type-2 Quinone Oxidoreductase (ndh-2) of *M. tuberculosis* (Developed Through Homology Modeling) | RMSD |
|---|---|---|
| Ala-319 | Ala-333 | 0.101 |
| Gln-320 | Gln-334 | 0.046 |
| Ile-321 | Gly-335 | 0.114 |
| Ala-322 | Ala-336 | 0.121 |
| Met-323 | Ile-337 | 0.148 |
| Gln-324 | Gln-338 | 0.151 |

## 10.10. Molecular Docking

Every molecule in the study was docked against the Mtb ndh-2 protein developed through homology modeling. The function of the ndh-2 enzyme/ protein can only be arrested, when the inhibitors bind to the quinone binding motif. Interestingly, all the molecules in the study entered the quinone binding tunnel to produce essential interactions with the quinone binding motif (formed by the residues Ala-333, Gln-334, Gly-335, Ala-336, Ile-337 & Gln-338). A critical hydrogen bond interaction was observed against Ala-333, the essential residue for effective binding of the substrate (quinone) to the motif (Fig. **5**). Docking score is imperative to understand how effective the inhibitors bind to the motif. The score varies between -5.8194 and -3.4273 Kcal/mol. The

**Table 7. Superimposition of the developed homology model against the protein structure of *C. thermarum* ndh-2.**

| Type-2 Quinone Oxidoreductase (ndh-2) of *C. thermarum* (PDB Code: 4NWZ) | Type-2 Quinone Oxidoreductase (ndh-2) of *M. tuberculosis* (Developed Through Homology Modeling) | RMSD |
|---|---|---|
| Ala-316 | Ala-333 | 0.117 |
| Gln-317 | Gln-334 | 0.338 |
| Ile-318 | Gly-335 | 0.254 |
| Ala-319 | Ala-336 | 0.344 |
| Ile-320 | Ile-337 | 0.423 |
| Gln-321 | Gln-338 | 0.558 |

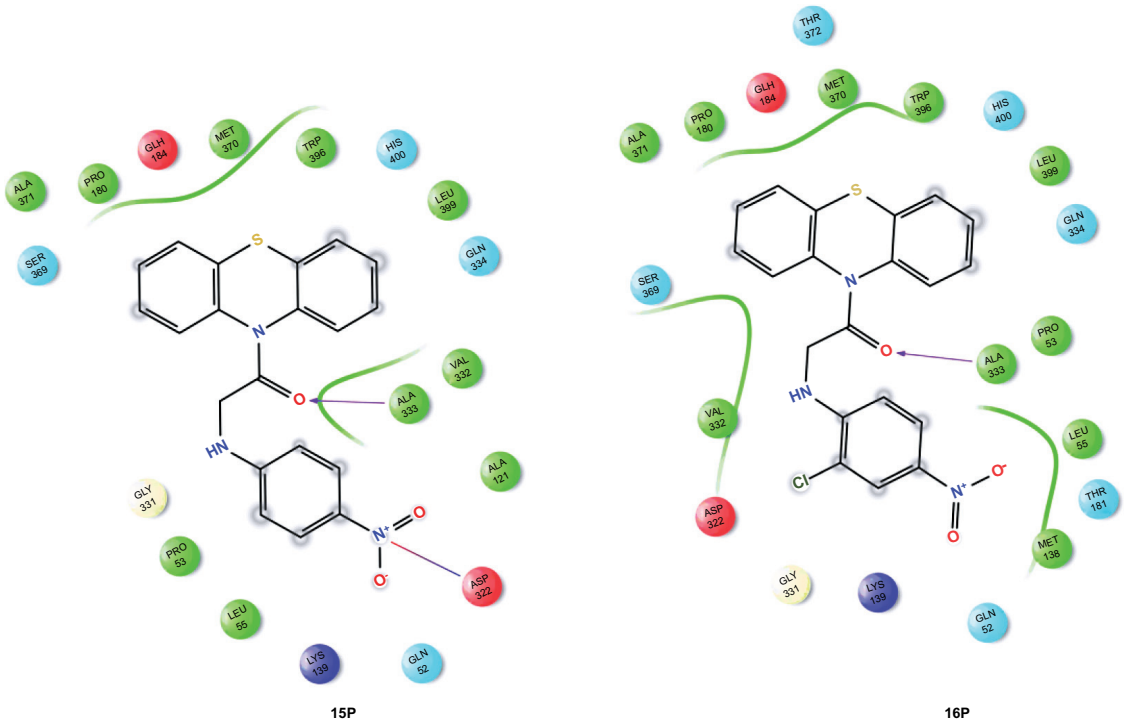


**Fig. (5).** Ligands 15p and 16p forming H-bond interaction with Ala-333 (a critical residue in quinone binding).

molecules 15c, 16c and 17c produced very good binding with minimum binding energy of -5.5957, -5.8194 and -5.7346 Kcal/mol, respectively (Table **8**) and a better correlation with antitubercular MIC was noticed. The developed molecules could inhibit ndh-2 and, thereby affecting the ATP synthesis to produce antimicrobial activity.

**Table 8. Docking of the tested molecules against Type-2 NADH dehydrogenase of Mtb.**

| S.No. | Ligand Code | Lowest Binding Energy (Kcal/mol) | Residues Forming the Quinone Binding Motif (Residues Producing H-bonding with the Ligand were Indicated in Bold) |
|---|---|---|---|
| 1 | 1p | -3.9931 | Ala-333,Gln-334,Gly-335, Ala-336,Ile-337,Gln-338 (no hydrogen bond interaction) |
| 2 | 2p | -4.2298 | **Ala-333**,Gln-334,Gly-335, Ala-336,Ile-337,Gln-338 |
| 3 | 3p | -4.2714 | **Ala-333**,Gln-334,Gly-335, Ala-336,Ile-337,Gln-338 |
| 4 | 4p | -4.2955 | **Ala-333**,Gln-334,Gly-335, Ala-336,Ile-337,Gln-338 |
| 5 | 5p | -4.3046 | **Ala-333**,Gln-334,Gly-335, Ala-336,Ile-337,Gln-338 |
| 6 | 6p | -4.3003 | **Ala-333**,Gln-334,Gly-335, Ala-336,Ile-337,Gln-338 |
| 7 | 7p | -4.3275 | **Ala-333**,Gln-334,Gly-335, Ala-336,Ile-337,Gln-338 |
| 8 | 8p | -4.2990 | **Ala-333**,Gln-334,Gly-335, Ala-336,Ile-337,Gln-338 |
| 9 | 9p | -4.3284 | **Ala-333**,Gln-334,Gly-335, Ala-336,Ile-337,Gln-338 |
| 10 | 10p | -4.6584 | **Ala-333**,Gln-334,Gly-335, Ala-336,Ile-337,Gln-338 |
| 11 | 11p | -4.6216 | **Ala-333**,Gln-334,Gly-335, Ala-336,Ile-337,Gln-338 |
| 12 | 12p | -4.7313 | **Ala-333**,Gln-334,Gly-335, Ala-336,Ile-337,Gln-338 |
| 13 | 13p | -4.6779 | **Ala-333**,Gln-334,Gly-335, Ala-336,Ile-337,Gln-338 |
| 14 | 14p | -5.4481 | **Ala-333**,Gln-334,Gly-335, Ala-336,Ile-337,Gln-338 |
| 15 | 15p | -5.5957 | **Ala-333**,Gln-334,Gly-335, Ala-336,Ile-337,Gln-338 |
| 16 | 16p | -5.8194 | **Ala-333**,Gln-334,Gly-335, Ala-336,Ile-337,Gln-338 |
| 17 | 17p | -5.7346 | **Ala-333**,Gln-334,Gly-335, Ala-336,Ile-337,Gln-338 |
| 18 | 18p | -4.1018 | Ala-333,Gln-334,Gly-335, Ala-336,Ile-337,Gln-338 (no hydrogen bond interaction) |
| 19 | 19p | -3.4273 | Ala-333,Gln-334,Gly-335, Ala-336,Ile-337,Gln-338 (no hydrogen bond interaction) |
| 20 | 20p | -3.5119 | Ala-333,Gln-334,Gly-335, Ala-336,Ile-337,Gln-338 (no hydrogen bond interaction) |

## CONCLUSION

The developed phenothiazine derivatives exhibited broad spectrum activity against *M. tuberculosis*, *S. aureus* and *E. coli*. The intact phenothiazine pharmacophore seems to be essential for both antitubercular and antibacterial activities.

Introduction of electron withdrawing groups at *meta* or *para* positions on the phenyl ring (compounds **14p, 15p, 16p)** significantly increased the activity in comparison to *ortho* substituted compounds (**3p & 18p**). Modifications introduced in the design of molecules were found to be appropriate, as the antitubercular activity improved with concurrent reduction of BBB permeability in comparison to chlorpromazine. The reduced binding of the molecules against dopamine receptor would also diminish the unwanted antipsychotic side effect. The molecules produced essential interactions with the residues forming quinone binding motif of Type-2 NADH dehydrogenase (ndh-2), thereby the ATP production could be arrested to exert antitubercular activity. Phenothiazines can be exploited in development of drugs for treating tubercular infections with no/ less antipsychotic effect.

## ETHICS APPROVAL AND CONSENT TO PARTICIPATE

Not applicable.

## HUMAN AND ANIMAL RIGHTS

No Animals/Humans were used for studies that are the basis of this research.

## CONSENT FOR PUBLICATION

Not applicable.

## CONFLICT OF INTEREST

The authors declare no conflict of interest, financial or otherwise.

## ACKNOWLEDGEMENTS

One of the authors (SS) acknowledges the financial support as Teaching Assistantship from MHRD, Govt. of India.

## REFERENCES

[1] Nguta, J.M.; Appiah-Opong, R.; Nyarko, A.K.; Yeboah-Manu, D.; Addo, P.G.A. Current perspectives in drug discovery against tuberculosis from natural products. *Int. J. Mycobacteriol.,* **2015**, *4*(3), 165-183.

[2] Lee, J.Y. Diagnosis and Treatment of Extrapulmonary Tuberculosis. *Tuberculosis Res. Dis.,* **2015**, *78*(2), 47-55.

[3] Organization, W.H. Global tuberculosis report 2016. **2016**.

[4] Martins, M.; Schelz, Z.; Martins, A.; Molnar, J.; Hajös, G.; Riedl, Z.; Viveiros, M.; Yalcin, I.; Aki-Sener, E.; Amaral, L. In vitro and *ex vivo* activity of thioridazine derivatives against *Mycobacterium tuberculosis*. *Int. J. Antimicrob. Agents,* **2007**, *29*(3), 338-340.

[5] Parrish, N.M.; Dick, J.D.; Bishai, W.R., Mechanisms of latency in *Mycobacterium tuberculosis*. *Trends in microbiol.,* **1998**, *6*(3), 107-112.

[6] Schaberg, T.; Bauer, T.; Castell, S.; Dalhoff, K.; Detjen, A.; Diel, R.; Greinert, U.; Hauer, B.; Lange, C.; Magdorf, K. [Recommendations for therapy, chemoprevention and chemoprophylaxis of tuberculosis in adults and children. German Central Committee against Tuberculosis (DZK), German Respiratory Society (DGP)]. *Pneumologie (Stuttgart, Germany),* **2012**, *66*(3), 133-171.

[7] Conover, M.S.; Hadjifrangiskou, M.; Palermo, J.J.; Hibbing, M.E.; Dodson, K.W.; Hultgren, S.J. Metabolic requirements of *Escherichia coli* in intracellular bacterial communities during urinary tract infection pathogenesis. *mBio,* **2016**, *7*(2), e00104-00116.

[8] Fellner, C. Companies Take Aim at MRSA Infections. *Pharm. Therap.,* **2016**, *41*(2), 126.

[9] Vesenbeckh, S.; Krieger, D.; Bettermann, G.; Schönfeld, N.; Bauer, T.T.; Rüssmann, H.; Mauch, H., Neuroleptic drugs in the treatment of tuberculosis: Minimal inhibitory concentrations of different phenothiazines against *Mycobacterium tuberculosis*. *Tuberculosis,* **2016**, *98*, 27-29.

[10] Maitra, A.; Bates, S.; Kolvekar, T.; Devarajan, P.V.; Guzman, J.D.; Bhakta, S. Repurposing-a ray of hope in tackling extensively drug resistance in tuberculosis. *Int. J. Infec. Dis.,* **2015**, *32*, 50-55.

[11] Amaral, L.; Boeree, M.J.; Gillespie, S.H.; Udwadia, Z.F.; Van Soolingen, D., Thioridazine cures extensively drug-resistant tuberculosis (XDR-TB) and the need for global trials is now! *Int. J. Antimicrob. Agents,* **2010**, *35*(6), 524-526.

[12] He, C.-X.; Meng, H.; Zhang, X.; Cui, H.-Q.; Yin, D.-L., Synthesis and bio-evaluation of phenothiazine derivatives as new anti-tuberculosis agents. *Chinese Chem. Lett.,* **2015**, *26*(8), 951-954.

[13] Amaral, L.; Kristiansen, J.E.; Viveiros, M.; Atouguia, J. Activity of phenothiazines against antibiotic-resistant *Mycobacterium tuberculosis*: A review supporting further studies that may elucidate the potential use of thioridazine as anti-tuberculosis therapy. *J. Antimicrob. Chemother.,* **2001**, *47*(5), 505-511.

[14] Feinberg, A.P.; Snyder, S.H. Phenothiazine drugs: structure-activity relationships explained by a conformation that mimics dopamine. *Proc. Natl. Acad. Sci. USA,* **1975**, *72*(5), 1899-1903.

[15] Jaszczyszyn, A.; Gąsiorowski, K.; Świątek, P.; Malinka, W.; Cieślik-Boczula, K.; Petrus, J.; Czarnik-Matusewicz, B., Chemical structure of phenothiazines and their biological activity. *Pharmacol. Rep.,* **2012**, *64*(1), 16-23.

[16] Madrid, P.B.; Polgar, W.E.; Toll, L.; Tanga, M.J. Synthesis and antitubercular activity of phenothiazines with reduced binding to dopamine and serotonin receptors. *Bioorg. Med. Chem. Lett.,* **2007**, *17*(11), 3014-3017.

[17] Kitchen, D.B.; Decornez, H.; Furr, J.R.; Bajorath, J. Docking and scoring in virtual screening for drug discovery: methods and applications. *Nat. Rev. Drug Dis.,* **2004**, *3*(11), 935.

[18] Satheeshkumar, S.; Amer, H.A.; Hojjat Ghasemi, G.; Gopal, N.; Sushil, K.S. Preliminary studies on ligand-based design and evaluation of new mycobacterial ATP synthase inhibitors. *Curr. Drug Ther.,* **2018**, *13*(1), 56-73.

[19] Lourenço, M.C.; de Souza, M.V.; Pinheiro, A.C.; Ferreira, M.d.L.; Gonçalves, R.S.; Nogueira, T.C.M.; Peralta, M.A., Evaluation of anti-tubercular activity of nicotinic and isoniazid analogues. *Arkivoc,* **2007**, *15*, 181-191.

[20] Bharti, S.K.; Nath, G.; Tilak, R.; Singh, S., Synthesis, anti-bacterial and anti-fungal activities of some novel Schiff bases containing 2, 4-disubstituted thiazole ring. *Eur. J. Med. Chem.,* **2010**, *45*(2), 651-660.

[21] Di, L.; Kerns, E.H.; Fan, K.; McConnell, O.J.; Carter, G.T., High throughput artificial membrane permeability assay for blood–brain barrier. *Eur. J. Med. Chem.,* **2003**, *38*(3), 223-232.

[22] Mosmann, T., Rapid colorimetric assay for cellular growth and survival: application to proliferation and cytotoxicity assays. *J. Immunol. Methods,* **1983**, *65*(1-2), 55-63.

[23] Hassan, F.; Abdul-Hameed, A.; Alshanon, A.; Abdullah, M.; Huri, H.Z.; Hairunisa, N.; Yousif, E. Antitumor activity for gold (III) complex by high content screening technique (HCS) and cell viability assay. *Asian J. Biochem.,* **2015**, *10*(6), 252.

[24] Sander, T.; Freyss, J.; von Korff, M.; Reich, J.R.; Rufener, C. OSIRIS, an entirely in-house developed drug discovery informatics system. *J. Chem. Infor. Mod.,* **2009**, *49*(2), 232-246.

[25] Maghrabi, A.H.; McGuffin, L.J., ModFOLD6: An accurate web server for the global and local quality estimation of 3D protein models. *Nucleic Acids Res.,* **2017**, gkx332.

[26] McGuffin, L.J.; Buenavista, M.T.; Roche, D.B., The ModFOLD4 server for the quality assessment of 3D protein models. *Nucleic Acids Res.,* **2013**, *41*(W1), W368-W372.

[27] Satheeshkumar, S.; Mohammad Faizan, B.; Ashok, K.; Gopal, N.; Sushil Kumar, S. Design, Synthesis and biological evaluation of carbazole derivatives as antitubercular and antibacterial agents. *Curr. Bioact. Comp.,* **2018**, *14*, 1-15.

[28] Lovell, S.C.; Davis, I.W.; Arendall, W.B.; de Bakker, P.I.; Word, J.M.; Prisant, M.G.; Richardson, J.S.; Richardson, D.C. Structure

validation by Cα geometry: ϕ, ψ and Cβ deviation. *Proteins: Str. Fun. Bioinform.,* **2003**, *50*(3), 437-450.

[29] Laskowski, R.A.; MacArthur, M.W.; Moss, D.S.; Thornton, J.M., PROCHECK: a program to check the stereochemical quality of protein structures. *J. App. Crystallography,* **1993**, *26*(2), 283-291.

[30] Colovos, C.; Yeates, T.O., Verification of protein structures: patterns of nonbonded atomic interactions. *Protein Sci.,* **1993**, *2*(9), 1511-1519.

[31] Eisenberg, D.; Lüthy, R.; Bowie, J.U., VERIFY3D: Assessment of protein models with three-dimensional profiles. *Meth. Enzymology,* **1997**, *277*, 396-404.

[32] Shen, J.; Zhang, W.; Fang, H.; Perkins, R.; Tong, W.; Hong, H., Homology modeling, molecular docking, and molecular dynamics simulations elucidated α-fetoprotein binding modes. *BMC Bioinformatics,* **2013**, *14*(14), S6.